Relating Microwave Modulation to Microbreaking Observed in Infrared Imagery

Ruth Branch, William J. Plant, *Member, IEEE*, Martin Gade, *Member, IEEE*, and Andrew T. Jessup, *Member, IEEE*

***Abstract*—Microwave modulation by swell waves and its relation to microbreaking waves were investigated in an ocean experiment. Simultaneous collocated microwave and infrared (IR) measurements of wind waves and swell on the ocean were made. The normalized radar cross section σ_o and the skin temperature $T_{\rm skin}$ were both modulated by the swell, but with differing phases. In general, σ_o maxima occurred on the front face, whereas $T_{\rm skin}$ maxima occurred on the rear face of the swell. Infrared imagery has shown that swell-induced microbreaking occurred at or near the swell crest and that the resulting warm wakes occurred on the rear face of the wave. When tilt and range modulations are taken into account, the location of microbreaking also accounts for the maximum of σ_o occurring on the front face of the swell. Thus, microbreaking waves generated near the crest of low-amplitude swell can produce microwave and IR signatures with the observed phase. The relationship between microwave and IR signals was further emphasized by comparing microwave Doppler spectra with simultaneous IR and visible images of the sea surface from the same location. When small and microscale breaking waves were present, Doppler spectra exhibited characteristics that are similar to those from whitecaps, having peaks with large Doppler offsets and polarization ratios near unity. When no microbreakers were present, Doppler offsets and polarization ratios were much smaller in accordance with a composite surface scattering theory.**

***Index Terms*—Infrared, microbreaking, microwave, ocean surface waves, swell modulation, wave breaking.**

I. Introduction

THE MODULATION of sea surface temperature and microwave backscatter by swell waves has been independently observed on the ocean [1], [2]. However, the extent to which the mechanisms that cause backscatter modulation are related to those for temperature modulation is unknown. The objectives of this letter are to investigate the relationship between the two types of modulation and to examine the mechanisms that are responsible for both phenomena. Collocated simultaneous microwave and infrared (IR) ocean measurements were made to reach these objectives.

Modulation of microwave backscatter by swell waves is a well-known phenomenon [2] and is composed of range, tilt, and hydrodynamic modulations [3]. Range and tilt modulations are due to the change in distance and orientation between the sensor and the surface as a wave propagates through the field of view (FOV). Hydrodynamic modulation characterizes how the wavenumber power spectrum is affected along the profile of swell waves. A weak hydrodynamic interaction theory predicts that the maximum modulation of small- to intermediate-scale gravity waves will occur near the crest of the swell, whereas capillary waves will be enhanced on the forward face near $\Psi = 90^\circ$ [4]. Hara and Plant [3] showed that tilt and range modulations shift the maximum of the measured microwave modulations about 45° farther toward the front face of the swell when it propagates toward the microwave antenna. Plant [5] developed a model to explain characteristics of the Doppler spectrum of microwave backscatter at large incidence angles by including Bragg scattering from bound tilted waves. He proposed that in addition to the modulated capillary and gravity–capillary waves, gravity waves with wavelength $O(1\ \text{m})$ may be modulated sufficiently by the swell to generate shorter waves bound to them. His model suggested that this occurs on the forward face of the swell at $\Psi = 130^\circ$. These short gravity waves with bound tilted shorter waves are suggestive of microbreaking waves [6], which are short gravity waves that break without entraining air. Microbreaking waves have a bore-like crest with parasitic capillary waves that ride along on the forward face and have been shown to produce an IR signature caused by disruption of the skin layer [7]–[9]. Thus, a primary motivation of this letter was to determine if the microwave scatterers proposed by Plant [5] are related to microbreaking that causes $T_{\rm skin}$ modulation.

Modulation of sea surface temperature has been observed on the ocean with IR instruments, and swell-induced microbreaking has been postulated as the cause of the modulation [1], [10]. The surface temperature measured by an IR radiometer corresponds to the so-called skin temperature $T_{\rm skin}$. The ocean thermal boundary, or skin, layer is $O(1\ \text{mm})$ thick, and the IR optical depth is $O(10\ \mu\text{m})$. $T_{\rm skin}$ within the wake of a breaking wave is approximately equal to the bulk temperature $T_{\rm bulk}$ because the breaking process mixes water from below to the surface [11], [12]. Thus, the skin temperature modulation due to breaking can be observed because $T_{\rm skin}$ inside the breaking wake area corresponds to $T_{\rm bulk}$, whereas $T_{\rm skin}$ outside the wake area corresponds to the undisturbed water temperature.

II. Ocean Measurements

Microwave scatterometer, IR, and video data were acquired during the Fluxes, Air–sea Interaction, and Remote Sensing

Manuscript received September 26, 2007; revised December 17, 2007. This work was supported in part by the Office of Naval Research.

R. Branch, W. J. Plant, and A. T. Jessup are with the Applied Physics Laboratory, University of Washington, Seattle, WA 98105 USA (e-mail: rbranch@apl.washington.edu; plant@apl.washington.edu; jessup@apl.washington.edu).

M. Gade is with the Center for Marine and Climate Research, University of Hamburg, 20146 Hamburg, Germany (e-mail: gade@ifm.uni-hamburg.de).

Digital Object Identifier 10.1109/LGRS.2008.916198

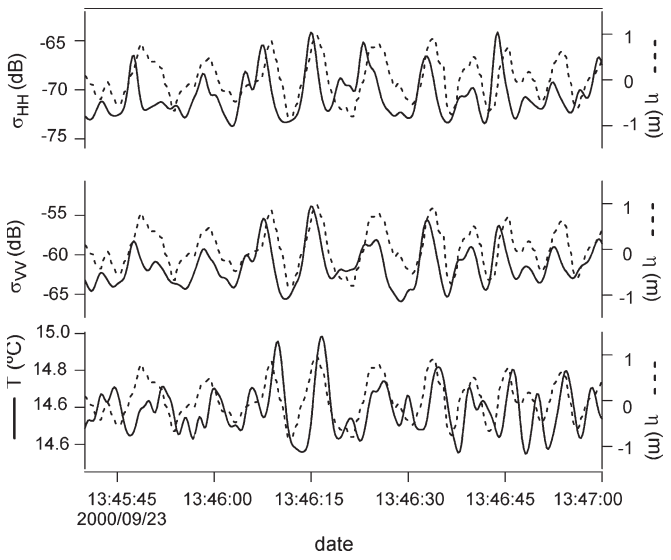

Fig. 1. Time series of field measurements showing coincident modulation of microwave cross section for VV and HH polarizations, ($\sigma_{\rm VV}$, middle and $\sigma_{\rm HH}$, top) and skin temperature ($T_{\rm skin}$, bottom). The surface displacement η is repeated as a dashed line with each variable. In general, the $T_{\rm skin}$ maxima occur on the rear face, whereas the σ maxima occur on the front face. The wind speed during this run was 2.25 m $\cdot$ s^{-1}.

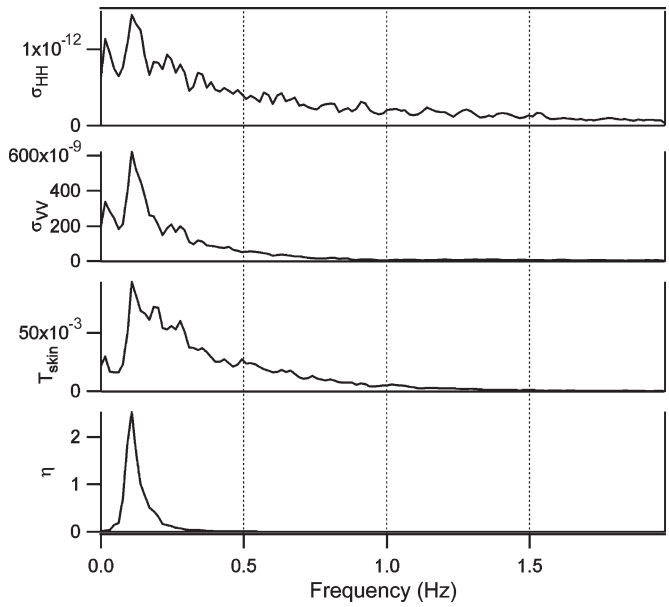

Fig. 2. Spectra of microwave cross sections, $T_{\rm skin}$, and surface displacement all show a peak at the swell frequency. These spectra correspond to the time series shown in Fig. 1.

(FAIRS) Experiment on the R/P Floating Instrument Platform (FLIP) in the Fall of 2000. A Ku-band microwave scatterometer, IR imager (3–5 μm), IR radiometer (9–11 μm), and a video camera were mounted on booms over the water and positioned with collocated FOVs. The scatterometer was mounted at an incidence angle of 70°, and the IR instruments at 33°. The sensors were pointed into the wind and remained so for the entire experiment since FLIP was freely floating. A full description of the experiment can be found in [13].

III. Results

The time series in Fig. 1 illustrates the modulation of $\sigma_{\rm VV}$ and $\sigma_{\rm HH}$, the normalized radar cross sections at vertical and horizontal polarizations, respectively, and $T_{\rm skin}$. The $T_{\rm skin}$ data are from the IR radiometer and correspond to the average temperature over a spot on the surface of roughly 30 cm in diameter. The surface displacement η measured by a sonic altimeter is superimposed as a dashed line on the other time series. The swell and wind waves were aligned, and the wind speed was 2.25 m $\cdot$ s^{-1}. The power spectra of $T_{\rm skin}$, $\sigma_{\rm VV}$, and $\sigma_{\rm HH}$ in Fig. 2 exhibit strong peaks at the swell frequency. In general, the maximum temperature appears on the rear face of the swell waves, whereas the cross-section maxima occur on the front face. Due to the environmental conditions, microwave backscatter was modulated much more frequently than temperature. This means that a statistical comparison of the phases cannot be made.

The association of whitecaps and large amplitude excursions in the radar cross section, or sea spikes, in moderate incidence angle measurements is well established [14], [15] and continues to be an area of active research [16]–[18]. The characteristics of backscatter associated with sea spikes due to breaking waves include a polarization ratio, $\sigma_{\rm HH}/\sigma_{\rm VV}$, near unity, a large Doppler frequency shift, and increased Doppler bandwidth [14]. The microwave signature of breaking over a wide range of scales is shown in Fig. 3 by comparing the Doppler spectra for VV and HH polarization with the simultaneous collocated IR and video imagery. The case of backscatter from the sea surface without wave breaking is shown in Fig. 3(a), in which the dotted ellipse on the IR image indicates the scatterometer's approximate FOV. In the absence of breaking, the Doppler spectra are characterized by $\sigma_{\rm HH}/\sigma_{\rm VV} < 1$ and nearly symmetric peaks with a small offset. The whitecap in Fig. 3(b), which appears warm in the IR image, produces Doppler spectra with $\sigma_{\rm HH}/\sigma_{\rm VV} \approx 1$ at higher frequencies and mean Doppler shifts that are significantly greater than zero. The spectra also show a significant return near zero frequency with $\sigma_{\rm HH}/\sigma_{\rm VV} < 1$, which corresponds to backscatter from the surface not affected by breaking. The white crest in the IR image is an apparent temperature increase due to the increased emissivity of foam [12]. The Doppler spectra from the much smaller whitecap shown in the IR sequence and video image in Fig. 3(c) are remarkably similar to those from the large whitecap in Fig. 3(b). The warm thermal signature of the wake left behind by the breaking process is apparent in the IR image. The final example is an IR image sequence in Fig. 3(d) showing the wake of a microbreaking wave, outlined by a dashed circle, which propagates through the images in time. Although the video image shows no visible signature, the Doppler spectra show a significant return with a large mean frequency, and $\sigma_{\rm HH}/\sigma_{\rm VV} \approx 1$. This example demonstrates that microbreaking waves produce microwave backscatter with characteristics that are similar to those from whitecaps. The environmental conditions during FAIRS limited the number of events like in [1]. This event is, therefore, an example of microwave backscatter from a microbreaking wave, but no statistical analysis can be performed on this data set.

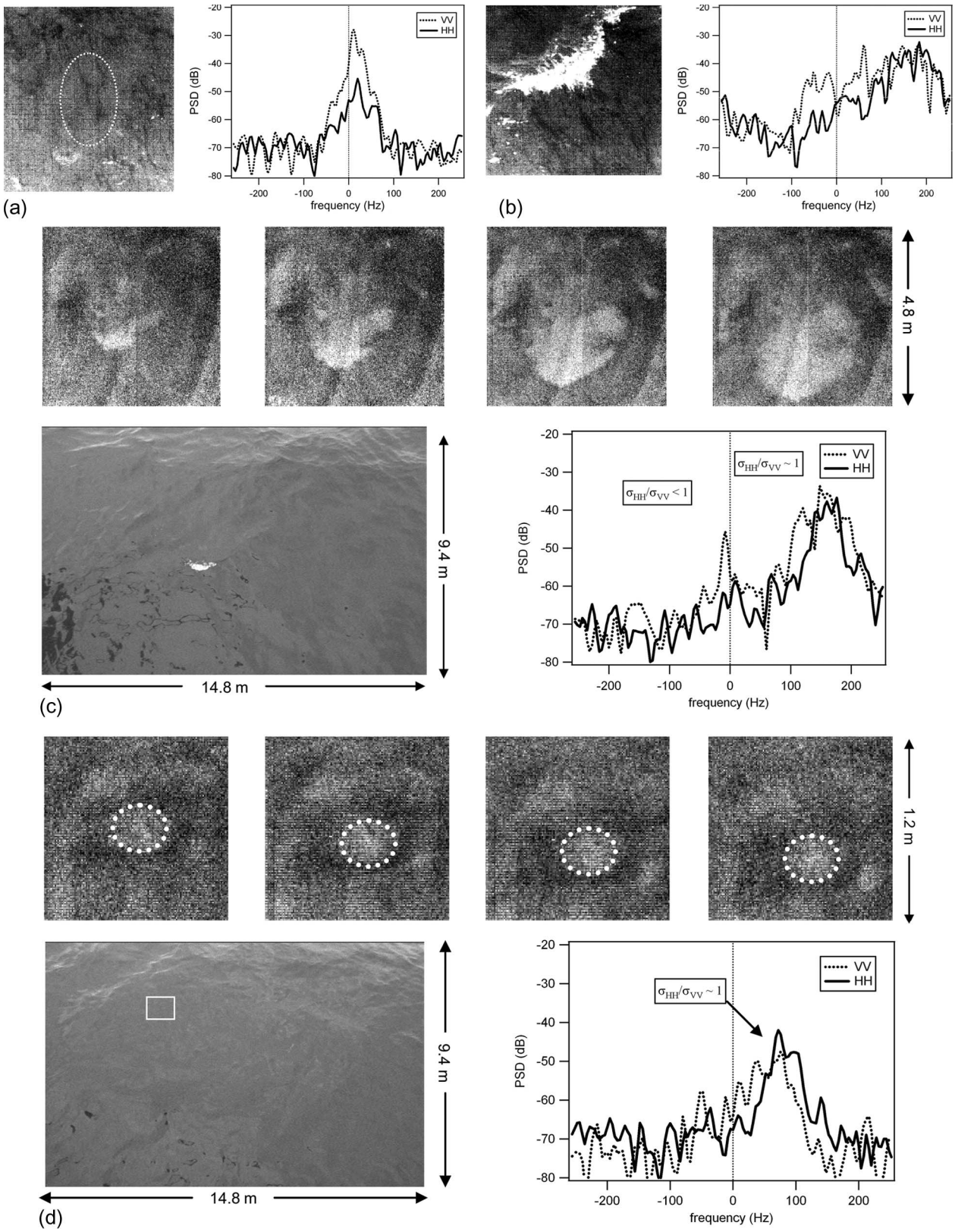

Fig. 3. Comparison of IR imagery (white is warm; black is cool), video imagery, and microwave spectral signatures of different scales of breaking during FAIRS with approximate wind speed of 5 m $\cdot$ s^{-1} and significant wave height of 0.75 m. (a) No breaking (IR and microwave): No distinct signature is apparent in the IR image, and the spectra show small Doppler shifts and $\sigma_{\mathrm{HH}}/\sigma_{\mathrm{VV}} < 1$. The 3-dB microwave spot is indicated in the IR image by the dashed ellipse. (b) A large whitecap (IR and microwave): The whitecap dominates the IR image, and the spectra show large Doppler shifts and $\sigma_{\mathrm{HH}}/\sigma_{\mathrm{VV}} \approx 1$. (c) A small whitecap (IR, video, and microwave): The whitecap is apparent in both the video and the IR images. The corresponding spectra have characteristics similar to those of the large whitecap. (d) A microscale breaking wave (IR, video, and microwave): The resulting warm wake is outlined by a dashed circle in the IR image, but no visible signature is seen in the video image (IR FOV is shown outlined in white). The spectra again show offset peaks with $\sigma_{\mathrm{HH}}/\sigma_{\mathrm{VV}} \approx 1$. All IR images are 4.8 m on a side except in (d) which are 1.2 m on side. Video images are 9.4 m $\times$ 14.8 m.

IV. Discussion and Conclusion

Modulation of microwave backscatter and sea surface temperature by swell waves was observed on the ocean. Microwave backscatter modulation was present more often than $T_{\rm skin}$ modulation. The presence of $T_{\rm skin}$ modulation is dependent on environmental conditions such as wave height, wind speed, bulk skin temperature difference, density of microbreaking waves, phase speed of the swell, and skin layer recovery time. The IR imagery showed that modulation of individual microbreaking waves was present even when their density was not high enough along the phase of the swell wave to be measured as a modulated signal by a radiometer [1].

Microwave cross-section maxima occurred on the forward face of the swell traveling toward the antenna, whereas the $T_{\rm skin}$ maxima occurred on the rear face. IR imagery showed that the swell-induced breaking occurred at or near the swell crest and that the resulting warm wakes occurred and persisted on the rear face of the wave [1]. This feature and the known shift of microwave modulation to the forward face due to tilt effects explain the different observed phases of the microwave and IR modulations. Phase shifts as large as those found by Plant [5] were not observed at the low wind speeds where IR effects could be measured.

Collocated simultaneous IR imagery and microwave Doppler spectra of breaking waves were compared for scales ranging from whitecaps to microbreakers. Consistent with previous investigations, the Doppler spectra corresponding to the whitecap exhibited peaks with a large Doppler offset and a polarization ratio near unity. A notable result was that Doppler spectra for small and microscale breaking waves exhibited similar characteristics. This result emphasizes the importance of including microscale wave breaking effects in models of microwave backscatter.

Collocated microwave and IR ocean measurements showed a simultaneous modulation by swell waves, which both could have been due to microbreaking waves. Further experiments should be carried out to statistically verify the phases of modulation under varying environmental conditions.

Acknowledgment

The authors would like to thank W. Keller and K. Hayes for the assistance with the microwave measurements.

References

[1] R. Branch and A. T. Jessup, "Infrared signatures of microbreaking wave modulation," *IEEE Geosci. Remote Sens. Lett.*, vol. 4, no. 3, pp. 372–376, Jul. 2007.

[2] W. C. Keller and W. J. Plant, "Cross sections and modulation transfer functions at L and Ku bands measured during the tower ocean wave and radar dependence experiment," *J. Geophys. Res.*, vol. 95, no. C9, pp. 16 277–16 289, Sep. 1990.

[3] T. Hara and W. J. Plant, "Hydrodynamic modulation of short wind-wave spectra by long waves and its measurement using microwave backscatter," *J. Geophys. Res.*, vol. 99, no. C5, pp. 9767–9784, 1994.

[4] R. Romeiser, A. Schmidt, and W. Alpers, "A three-scale composite surface model for the ocean wave-radar modulation transfer function," *J. Geophys. Res.*, vol. 99, no. C5, pp. 9785–9801, 1994.

[5] W. J. Plant, "A model for microwave Doppler sea return at high incidence angles: Bragg scattering from bound, tilted waves," *J. Geophys. Res.*, vol. 102, no. C9, pp. 21 131–21 146, 1997.

[6] M. L. Banner and O. M. Phillips, "On the incipient breaking of small scale waves," *J. Fluid Mech.*, vol. 77, pp. 825–842, 1974.

[7] A. T. Jessup, C. J. Zappa, and H. Yeh, "Defining and quantifying microscale wave breaking with infrared imagery," *J. Geophys. Res.*, vol. 102, no. C10, pp. 23 145–23 153, 1997.

[8] C. J. Zappa, W. E. Asher, and A. T. Jessup, "Microscale wave breaking and air-water gas transfer," *J. Geophys. Res.*, vol. 106, no. C5, pp. 9385–9392, 2001.

[9] C. J. Zappa, W. E. Asher, A. T. Jessup, J. Klinke, and S. R. Long, "Microbreaking and the enhancement of air-water gas transfer velocities," *J. Geophys. Res.*, vol. 109, no. C8, C08 S16, 2004. DOI:10.1029/2003JC001897.

[10] A. T. Jessup and V. Hesany, "Modulation of ocean skin temperature by swell waves," *J. Geophys. Res.*, vol. 101, no. C3, pp. 6501–6511, 1996.

[11] K. B. Katsaros, "The aqueous thermal boundary layer," *Bound.-Layer Meteorol.*, vol. 18, no. 1, pp. 107–127, Feb. 1980.

[12] A. T. Jessup, C. J. Zappa, M. R. Loewen, and V. Hesany, "Infrared remote sensing of breaking waves," *Nature*, vol. 385, no. 6611, pp. 52–55, Jan. 1997.

[13] R. Fogelberg, "A study of microbreaking modulation by ocean swell using infrared and microwave techniques," M.S. thesis, Dept. Civil Environ. Eng., Univ. Washington, Seattle, WA, 2003.

[14] A. T. Jessup, W. Melville, and W. Keller, "Breaking waves affecting microwave backscatter 1. Detection and verification," *J. Geophys. Res.*, vol. 96, no. C11, pp. 20 547–20 559, Nov. 1991.

[15] P. H. Y. Lee, J. D. Barter, K. L. Beach, C. L. Hindman, B. M. Lake, H. Rungaldier, J. C. Shelton, A. B. Williams, R. Yee, and H. C. Yuen, "X band microwave backscattering from ocean waves," *J. Geophys. Res.*, vol. 100, no. C2, pp. 2591–2611, 1995.

[16] E. Ericson, D. Lyzenga, and D. Walker, "Radar backscatter from stationary breaking waves," *J. Geophys. Res.*, vol. 104, no. C12, pp. 29 679–29 695, 1999.

[17] E. Dano, D. Lyzenga, and M. Perlin, "Radar backscatter from mechanically generated transient breaking waves—Part I: Angle of incidence dependence and high resolution surface morphology," *IEEE Trans. Geosci. Remote Sens.*, vol. 26, no. 2, pp. 181–200, Apr. 2001.

[18] M. Haller and D. Lyzenga, "Comparison of radar and video observations of shallow water breaking waves," *IEEE Trans. Geosci. Remote Sens.*, vol. 41, no. 4, pp. 832–844, Apr. 2003.